

Growth and characterization of ZnO needles

Wei Feng · Jie Chen · Chun-yan Hou

Received: 30 July 2012 / Accepted: 2 November 2012 / Published online: 20 November 2012
© The Author(s) 2012. This article is published with open access at Springerlink.com

Abstract ZnO needles were synthesized by vapor-phase transport method, and the microstructure and room temperature photoluminescence properties were characterized by scanning electron microscopy (SEM), Fourier transform infrared spectroscopy (FT-IR), X-ray diffraction (XRD), transmission electron microscope (TEM) and UV microlaser Raman spectrometer. The SEM image indicated that the products prepared had tetrapod-like structures. The results of FT-IR and XRD revealed that they were single crystalline with the hexagonal wurtzite structure. The TEM and high-resolution TEM images indicated that ZnO needles were single crystalline and grew along the direction of (001). The room temperature photoluminescence spectra of the products exhibited a strong ultraviolet emission band at 375 nm and very broad weak green luminescence band at 510 nm.

Keywords ZnO · Nanoneedles · Microstructure · Vapor-phase transport

Introduction

ZnO as a wide band gap semiconductor (energy gap of 3.35 eV at room temperature) has been focused on the

promising application as ultraviolet (UV) light-emitting diodes and laser diodes (Pacholski and Kornowski 2004; Singh 2010). Various methods, such as precipitation (Lee et al. 2002), sol-gel (Rani et al. 2008), vapor-liquid-solid (VLS) growth (Ham et al. 2005), chemical vapor deposition (CVD) (Zeng and Ye 2005), thermal decomposition (Zhao et al. 2007), metal organic vapor-phase epitaxy (Li et al. 2000), have been developed for controlling ZnO structures, since its various properties strongly depend on its structures including the crystal size, orientation, morphology, aspect ratio and even crystalline density. Currently, many interesting ZnO nanostructures including nanorods (Lucas and Mai 2007), nanowires (Xiang et al. 2007), tetrapods (Chen et al. 2007), nanocombs (Li et al. 2008), nanotubes (Anas and Mangalaraja 2010), nanopen-cils (Shen et al. 2006) and star-like (Peng et al. 2010) have been successfully synthesized. In this letter, we presented a simple vapor-phase transport method approach to fabricate ZnO needles. The microstructure and room temperature photoluminescence (PL) properties were also investigated.

Experimental

Preparation of ZnO

Zinc acetate $[(\text{CH}_3\text{COO})_2\text{Zn}\cdot\text{H}_2\text{O}]$, from Aldrich] and the sodium dodecyl benzene sulfonate ($\text{C}_{18}\text{H}_{29}\text{NaO}_3\text{S}$, from Aldrich) were dissolved in deionized water at different concentration of 0.1 and 0.2 mol/L, respectively. Then, certain volume zinc acetate solution was slowly added to sodium dodecyl benzene sulfonate solution under vigorous stirring at room temperature for 15 min. The samples were filtrated and washed with distilled water several times. Finally, the samples were dried in air at 378 K for 4 h,

W. Feng (✉) · C. Hou
Key Lab of Groundwater Resources and Environment,
Ministry of Education, Jilin University, Jiefang Road 2519,
Changchun 130021, People's Republic of China
e-mail: weifeng@dmlu.edu.cn

J. Chen
Key Laboratory of Industrial Ecology and Environmental
Engineering (MOE), School of Environmental Science
and Technology, Dalian University of Technology,
Linggong Road 2, Dalian 116024, People's Republic of China

which was noted as organic-Zn. The organic-Zn samples were placed in a crucible with glass substance as a cover. The regular air holes with 0.3 mm diameter and 2 mm distance were distributed uniformly in the surface of substrates. The ZnO samples were obtained by calcined at 1223 K for 6 h.

Instrumental analysis

FT-IR spectra of samples deposited on KBr pellets were determined at room temperature with a Nicolet Impact 550 FT-IR spectrometer in the range of 4000–400 cm^{-1} . XRD patterns were measured using a Rigaku D/MAX-3A X-ray diffractometer at a scanning rate of 4° per min with 2θ ranging from 20° to 80° , using Cu $K\alpha$ radiation ($\lambda = 1.5418 \text{ \AA}$). The overview morphology of samples was obtained on a PHILIPS XL-30 scanning electron microscopy (SEM). The TEM images of the samples were obtained on a JEOL JEM-200CX transmission electron microscope by dropping complex solution onto copper grids. The high-resolution TEM (HRTEM) images were obtained by analytical transmission electron microscope (H-600 TEM). In order to study the luminescent properties, the samples were excited by 325 nm line of the He-Cd laser with a power of 50 mW. The laser beam was focused to a spot of 30 μm . The luminescence signals were acquired by a UV microlaser Raman spectrometer.

Results and discussion

FT-IR spectra of organic-Zn and ZnO needles are shown in Fig. 1. The curve (a) shows the peaks of the organic-Zn samples. The broad peak in the range 3300–3500 cm^{-1} was due to the hydrated water presented in organic-Zn. The peaks near 2920 and 2838 cm^{-1} ascribed to asymmetric and symmetric of C–H bond. The absorption peak at 1500 cm^{-1} belongs to the vibration of (C=O), whereas the one at 1400 cm^{-1} was the scissoring vibration of CH_2 . The peak at 1046 cm^{-1} can be assigned to the deformation vibration of C=O. The intensity of these peaks decreased and disappeared, indeed, after annealing (as shown in the curves b). A new peak around 470 cm^{-1} appeared, which was assigned to the stretching mode of ZnO (Jiménez 1998). Band at 3421 cm^{-1} (H–O–H stretching) was due to the presence of adsorbed water, and peak at around 1635 cm^{-1} ascribed to bending vibrations of water owing to the OH group on ZnO-particles surface adsorbed from the atmosphere.

The crystal structure of organic-Zn and ZnO needles was examined with XRD (as shown in Fig. 2). Compared with organic-Zn, all the diffraction peaks of the as-obtained materials can be well indexed to the hexagonal phase ZnO

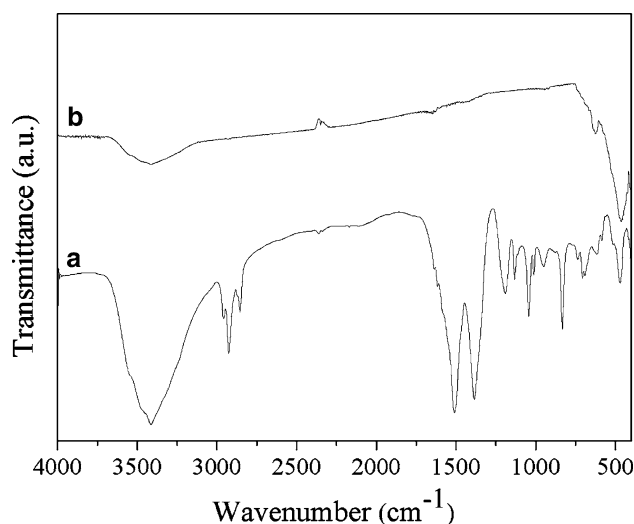


Fig. 1 FT-IR spectra of organic-Zn (a) and ZnO needles (b)

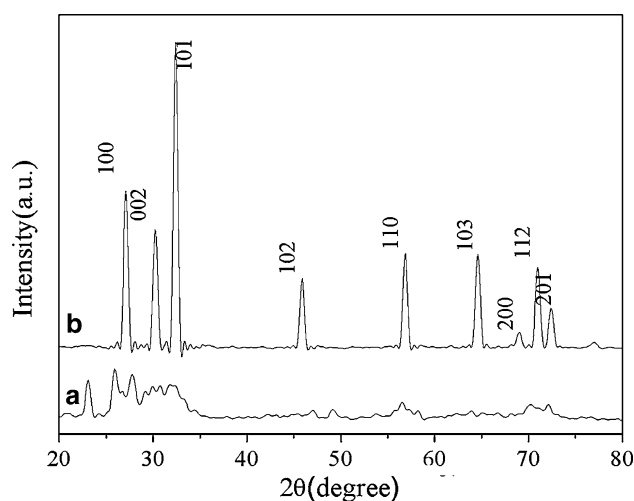


Fig. 2 XRD patterns of organic-Zn (a) and ZnO needles (b)

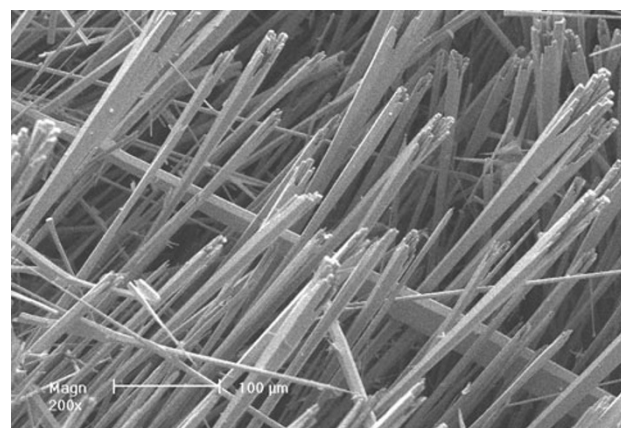


Fig. 3 SEM image of ZnO needles

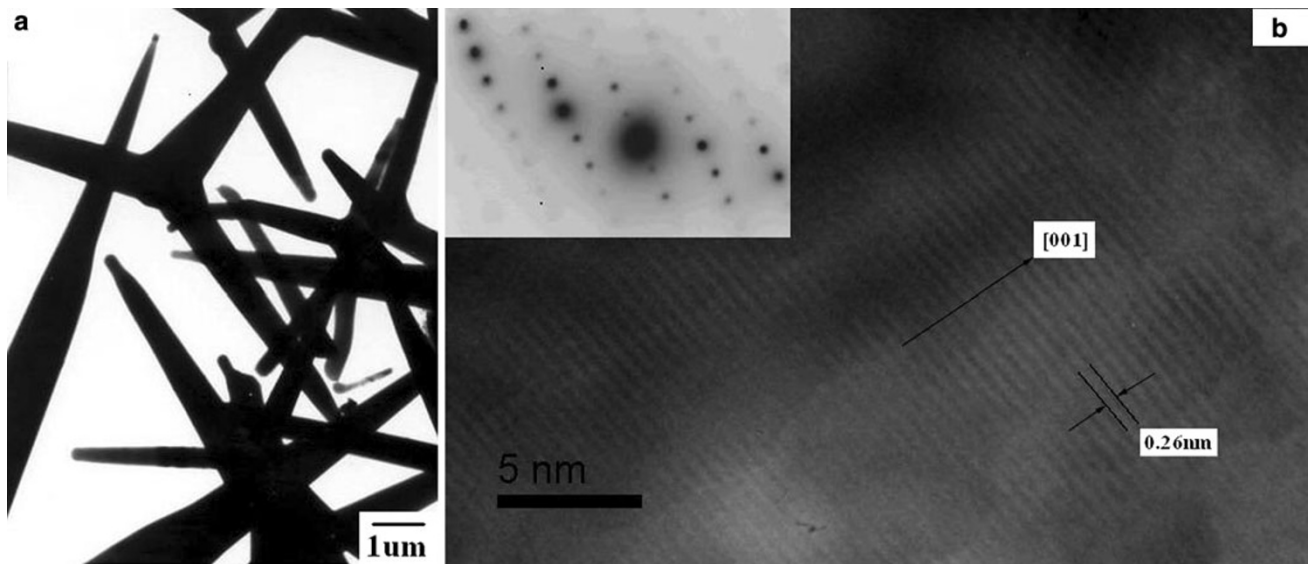


Fig. 4 TEM image of ZnO needles (a), HRTEM image of ZnO needles (b) and the insert shows the SAED pattern

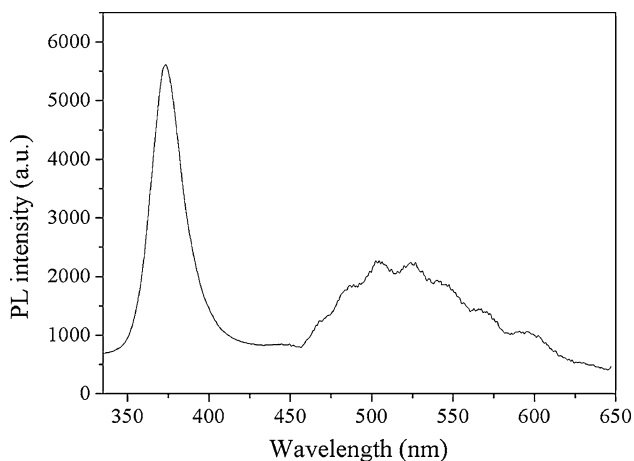


Fig. 5 PL spectrum of ZnO needles

with lattice constants $a = 3.242 \text{ \AA}$ and $c = 5.194 \text{ \AA}$ (JCPDS card No. 79-0205). The results indicated that ZnO samples consisted of pure phase, and no characteristic peaks were observed for other impurities. The sharp peaks demonstrated that ZnO samples were well crystallized.

Figure 3 shows the low-magnification SEM image of ZnO samples. It revealed that needle-like ZnO crystals with many stacked together, the whole size of which was in the range of $500 \mu\text{m}$ and thickness was about $5\text{--}10 \mu\text{m}$, vertically stood on the surface of substrates.

The general TEM micrograph of the ZnO samples is shown in Fig. 4a. It demonstrated that the products mainly consisted of solid needle-like structure. The diameter of the products ranged from 5 to $20 \mu\text{m}$ and the length was up to $500 \mu\text{m}$, which agreed with the SEM results. Figure 4b confirmed a single ZnO particle, which had smooth face,

extending outside continuously without curving and clearly showing needle-shaped feature. The insert selected area electron diffraction (SAED) pattern taken on the needle-like ZnO exhibited the oriented growth direction along the c -axis. Different parts of this whisker showed exactly the same electron pattern indicating the single crystallinity of the whole single whisker. Dozens of individual whiskers have been examined using this method, and confirmed the single crystallinity.

Structurally, as reported, the wurtzite hexagonal ZnO crystal was composed of O^{2-} and Zn^{2+} ions, arranged in a tetrahedral manner and stacked alternatively along the c -axis direction. It has been proved that the growth of ZnO crystals was the fastest in the (001) surfaces due to its self-catalytic property, as compared to any other growth facets (Wang and Kong 2003). Accordingly, ZnO particles with high aspect ratio were obtained. Figure 4c shows the HRTEM image of the ZnO products. It revealed that ZnO had a clear and structurally perfect surface. The adjacent lattice plane (arrow-heads) was about 0.26 nm , which corresponded to the distance between two (002) planes. The clear lattice fringes in the HRTEM image indicated that the individual ZnO was single crystal structure. The (002) planes were perpendicular to the growth direction of ZnO, which indicated that ZnO grew along the (001) direction (c -axis).

To study the optical properties and crystal defects of ZnO microstructures, room temperature PL spectrum was measured and the typical spectrum is shown in Fig. 5. It was well known that ZnO crystal exhibited two emission peaks when excited with UV light. One was at about 370 nm (so-called UV luminescence band), and the other was near 530 nm (so-called green luminescence band). In

our experiment, peak at 375 nm, corresponding to the near band edge emission, related to the direct recombination of photogenerated electron–hole pairs between the ZnO band gaps. For the green emission, the very broad, weak peak was located at 510 nm, which revealed the existence of a low concentration of oxygen vacancies.

Conclusion

In summary, large quantity and single crystalline ZnO needles have been prepared through a simple vapor-phase transport method. Needle-like ZnO samples were wurtzite hexagonal structures. PL spectrum exhibited two emission bands, which may be contributed by the near band edge emission and green emission. In addition, we believed that this simple process can also be applied to synthesize other metal oxide for functional materials.

Acknowledgments This work was financially supported by the National Science Foundation of China (No. 20977012).

Open Access This article is distributed under the terms of the Creative Commons Attribution License which permits any use, distribution, and reproduction in any medium, provided the original author(s) and the source are credited.

References

- Anas S, Mangalaraja RV, Ananthakumar S (2010) Studies on the evolution of ZnO morphologies in a thermohydrolysis technique and evaluation of their functional properties. *J Hazard Mater* 175:889–895
- Chen ZG, Ni A, Li F, Cong HT, MCheng H, Lu GQ (2007) Synthesis and photoluminescence of tetrapod ZnO nanostructures. *Chem Phys Lett* 434:301–305
- Ham H, Shen GZ, Cho JH, Lee TJ, Seo SH, Lee CJ (2005) Vertically aligned ZnO nanowires produced by a catalyst-free thermal evaporation method and their field emission properties. *Chem Phys Lett* 40:469–473
- Jiménez AE, Soto Urueta JA, Suárez-Parra R (1998) Optical and electrical characteristics of aluminum-doped ZnO thin films prepared by solgel technique. *J Cryst Growth* 192:430–438
- Lee CJ, Lee TJ, Lyu SC, Zhang Y, Ruh H, Lee HJ (2002) Field emission from well-aligned zinc oxide nanowires grown at low temperature. *Appl Phys Lett* 19:3648–3650
- Li Y, Meng GW, Zhang LD, Phillipp F (2000) Ordered semiconductor ZnO nanowire arrays and their photoluminescence properties. *Appl Phys Lett* 76:2011–2013
- Li C, Yu ZS, Fang SM, Wang HX, Gui YH, Xu JQ, Chen RF (2008) Fabrication and gas sensing property of honeycomb-like ZnO. *Chinese chem Lett* 19:599–603
- Lucas M, Mai W, Yang K (2007) Aspect ratio dependence of the elastic properties of ZnO nanobelts. *Nano Lett* 7:1314–1317
- Pacholski C, Kornowski A, Weller H (2004) Site-specific photodeposition of silver on ZnO nanorods. *Angew Chem* 116:4878–4881
- Peng ZW, Dai GZ, Chen P, Zhang QL, Wan Q, Zou BS (2010) Synthesis, characterization and optical properties of star-like ZnO nanostructures. *Mater Lett* 64:898–902
- Rani S, Suri P, Shishodia PK, Mehra RM (2008) Synthesis of nanocrystalline ZnO powder via sol-gel route for dye-sensitized solar cells. *Sol Energy Mater Sol Cells* 92:1639–1645
- Shen G, Bando Y, Liu B, Golberg D, Lee CJ (2006) Characterization and field-emission properties of vertically aligned ZnO nanonails and nanopencils fabricated by a modified thermal-evaporation process. *Adv Funct Mater* 16:410–416
- Singh AK (2010) Synthesis, characterization, electrical and sensing properties of ZnO nanoparticles. *Adv Powder Technol* 21:609–613
- Wang ZL, Kong XY, Zuo JM (2003) Induced growth of asymmetric nanocantilever arrays on polar surfaces. *Phys Rev Lett* 91:5502–5505
- Xiang Q, Pan QY, Xu JQ, Shi LY, Xu PC, Liu PC (2007) Solvothermal synthesis of ZnO nanowires. *Chinese J Inorg Chem* 23:369–374
- Zeng YJ, Ye ZZ, Xu WZ (2005) Well-aligned ZnO nanowires grown on Si substrate via metal-organic chemical vapor deposition. *Appl Surf Sci* 250:280–283
- Zhao JW, Qin LR, Xiao ZD, Zhang LD (2007) Synthesis and characterization of novel flower-shaped ZnO nanostructures. *Mater Chem Phys* 105:194–198